Regular Article

Microwave-Assisted Synthesis, Molecular Docking, and Cholinesterase Inhibitory Activities of New Ethanediamide and 2-Butenediamide Analogues

Mehmet Koca,[a] Kadir Ozden Yerdelen,*[,a] Baris Anil,[b] and Zeynep Kasap[a]

[a] *Department of Pharmaceutical Chemistry, Faculty of Pharmacy, Ataturk University; Erzurum 25240, Turkey: and* [b] *Department of Organic Chemistry, Faculty of Science, Ataturk University; Erzurum 25240, Turkey.*
Received October 31, 2014; accepted December 25, 2014

A novel series of *meta*-substituted ethanediamide and 2-butenediamide derivatives were synthesized and tested for their ability to inhibit electric eel acetylcholinesterase (AChE) and equine serum butyrylcholinesterase (BuChE). The synthesized compounds were evaluated against ChE enzymes using the colorimetric method described by Ellman *et al.* (*Biochem. Pharmacol.*, 7, 1961). It was revealed that some synthesized compounds exhibited high anticholinesterase activity, among which compounds 1f and 2f were the most active inhibitors against BuChE (IC_{50} value=1.47 μM) and AChE (IC_{50} value=2.09 μM), respectively. Docking simulations revealed that the inhibitors 1f and 2f are capable of simultaneously binding the peripheral anionic site as well as the catalytic anionic site of both ChE enzymes. These derivatives are considered interesting candidates for Alzheimer's disease treatment.

Key words ethanediamide; 2-butenediamide; anticholinesterase activity; molecular docking

Alzheimer's disease (AD), the most common cause of dementia is an irreversible neurodegenerative disorder characterized by the loss of memory, learning and inability to perform routine activities.[1–4] The progression and definite reasons of the AD are still mostly unknown, but the most favourite hypotheses have been put forward on the basis of the various causative factors such as cholinergic, amyloid, tau and metal hypothesis.[5] The standard medical treatment for AD includes cholinesterase inhibitors (ChEIs) and a partial *N*-methyl-D-aspartate (NMDA) antagonists.[6,7] The cholinergic hypothesis is one of the oldest and most popular hypotheses outlining the pathogenesis of AD. Acetylcholine (ACh) deficiency severely affects the cognitive abilities, memory function and emotional responses in AD patients.

According to the cholinergic hypothesis, the main approach of the current pharmacotherapy for AD is increasing the levels of ACh through the inhibition of cholinesterase enzymes (ChEs).[8,9] Two major cholinesterases, acetylcholinesterase (AChE) and butyrylcholinesterase (BuChE), which are located in the central nervous system (CNS), are able to hydrolyse the neurotransmitter ACh.[10] Studies have indicated that AD is defined by decrement of level of AChE in the early stages of the disease along with the increasing ratio of BuChE to AChE in advanced stages of the disease.[11] Furthermore, BuChE has been found capable of compensating for the missing AChE catalytic functions in the synaptic cleft and its activity increases, 30–60%, during AD.[12–15] Due to the role of BuChE in the hydrolysis of ACh, the inhibition of both ChEs using a dual inhibitor should result in increased levels of ACh in the brain that provides more successful clinical efficacy of AD.[16,17] High levels of metals like mercury cause severe and fatal neurologic diseases, as well as learning and memory problems and movement disorders.[18] Imbalances in the levels and distribution of these metals in the brain, especially zinc, copper and iron may play a role in dementias like Alzheimer's disease (the so-called "metal hypothesis").[19] The level of metal ions (Fe^{2+}, Cu^{2+}, Zn^{2+}) in AD patients is 3–7 times higher than the level in healthy individuals.[20]

In our previous studies, we determined the significant effects of the synthesized compounds, which have different halogen atoms (F, Cl, Br, I) on *meta*- and *para*-positions of aniline rings, on acetyl- and butyryl-cholinesterase inhibition.[21,22] In this context, we investigated some potential positive contributions to cholinesterase inhibitory activity by addition a chloro atom to the *para* position of benzyl ring and we report the synthesis of new ethanediamide and 2-butenediamide analogues and their *in vitro* cholinesterases inhibitory activities. Molecular docking and metal chelation studies were also conducted for the most potent derivatives.

Results and Discussion

Chemistry As depicted in Chart 1, intermediate starting compounds, 4-chlorobenzyl-(3-substituted-phenyl)-amines, required for the synthesis of ethanediamide and 2-butenediamide derivatives were obtained by using microwave irradiation under solvent-free phase-transfer catalysis conditions after a short reaction time (5 min). A same synthetic procedure was used for the synthesis of some *meta*-substituted benzanilines which was reported in our previous study.[21] 3-Substituted ethanediamides (**1a**–**f**) were synthesized by the reaction of oxalyl chloride with 4-chlorobenzyl-(3-substituted-phenyl)-amines in tetrahydrofuran in the presence of triethylamine (TEA) with moderate to good yields (14–81%). 2-Butenediamide derivatives (**2a**–**f**) were obtained in moderate yields (13–66%) by following the same procedure described in the previously reported literature.[22] The obtained spectroscopic data are in accordance with the predicted structures. The synthesis scheme of the compounds is presented in Chart 1. In the proton nuclear magnetic resonance (^{1}H-NMR) spectra, the resonance signals of ethylene bridge protons are registered as singlets in the range of 6.83 to 7.04 ppm for the compounds **2a**–**f**. The signals for the aromatic protons were showed in

* To whom correspondence should be addressed. e-mail: dadasozden@gmail.com

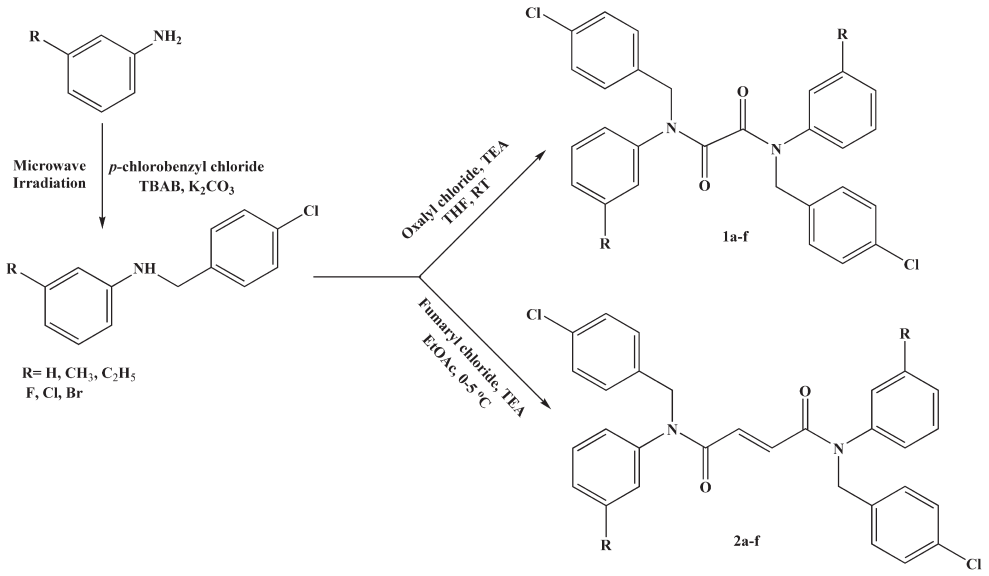

Chart 1. Synthesis of Ethanediamide (**1a**–**f**) and 2-Butenediamide (**2a**–**f**) Derivatives

Table 1. *In Vitro* Inhibitory Potential of Target Compounds **1a**–**f** and **2a**–**f** against AChE and BuChE

Compound	R	IC_{50} (μM)		Selectivity index[c]
		AChE[a]	BuChE[b]	
1a	H	> 100	1.74±0.01	53.76
1b	CH_3	> 100	12.04±0.11	8.30
1c	C_2H_5	> 100	17.11±0.14	5.84
1d	F	> 100	4.78±0.07	20.92
1e	Cl	> 100	3.16±0.08	31.64
1f	Br	> 100	1.47±0.10	68.02
2a	H	3.51±0.03	> 100	0.02
2b	CH_3	30.00±0.13	11.22±0.02	2.67
2c	C_2H_5	19.18±0.02	35.48±0.24	0.37
2d	F	15.13 ±0.13	> 100	0.15
2e	Cl	7.94±0.02	> 100	0.08
2f	Br	2.09±0.18	> 100	0.03
Neostigmin		6.76±0.01	14.45±0.01	2.13
Ambenonium		4.07±0.06	6.02±0.04	1.48

a) Fifty percent inhibitory concentration (means±S.D. of three experiments) of AChE. *b*) Fifty percent inhibitory concentration (means±S.D. of three experiments) of BuChE. *c*) Selectivity for BuChE=IC_{50} (AChE)/IC_{50} (BuChE).

the range of δ 6.62–7.52 ppm and δ 6.72–7.49 ppm for the compounds **1a**–**h** and **2a**–**h**, respectively. The N-CH_2 protons appeared at δ 4.61–4.64 ppm for the compounds **1a**–**h** and δ 4.83–4.85 ppm for the compounds **2a**–**h**. The carbon nuclear magnetic resonance (^{13}C-NMR) spectrum shows characteristic carbon resonance frequencies of carbonyl atoms in the range of $\boldsymbol{\delta}$ 163.77–164.44 ppm for the compounds **1a**–**h** and δ 163.97–164.42 ppm for the compounds **2a**–**h**. The aromatic carbons appeared at δ 122.46–145.39 ppm for the compounds **1a**–**h** and δ 115.49–146.20 ppm for the compounds **2a**–**h**. N-CH_2 groups appeared at δ 51.32–51.41 ppm. In the positive electron impact (EI) mass spectra, the molecular ion peaks [M+H] show that the predicted compound has formed.

Cholinesterase Inhibitory Activity The inhibitory activity of the compounds against AChE and BuChE was measured according to the colorimetric assay of Ellman *et al.*[23] Neostigmine and ambenonium were used as the reference compounds. The IC_{50} values of all tested compounds and their selectivity index for BuChE are summarized in Table 1. All butenediamide derivatives **2a**–**f** showed moderate to good inhibitory activity on AChE with micromolar concentrations. The *meta* bromo-substituted compound among the butenediamide derivatives, **2f** (IC_{50}=2.09 μM), showed the most potent inhibitory activity against AChE, being 3.23- and 1.94-fold stronger than the reference compounds neostigmine bromide (IC_{50}=6.76 μM) and ambenonium dichloride (IC_{50}=4.07 μM), respectively. The other compound in the series, **2a**, was found the second most powerful compound with IC_{50} value of 3.51 μM. Also, the most potent compounds, **2a** and **2f**, were found more selective inhibitors on AChE than the other compounds with the lowest selectivity index (SI) values against BuChE (0.02, 0.03, respectively). The compounds **2b**–**e** showed a moderate inhibitory activity to the reference compounds. Only the compounds, (**2b**, **2c)**, showed a moderate inhibitory activity on BuChE with IC_{50} values of 11.22 and 35.48 μM.

All ethanediamide compounds showed moderate to high

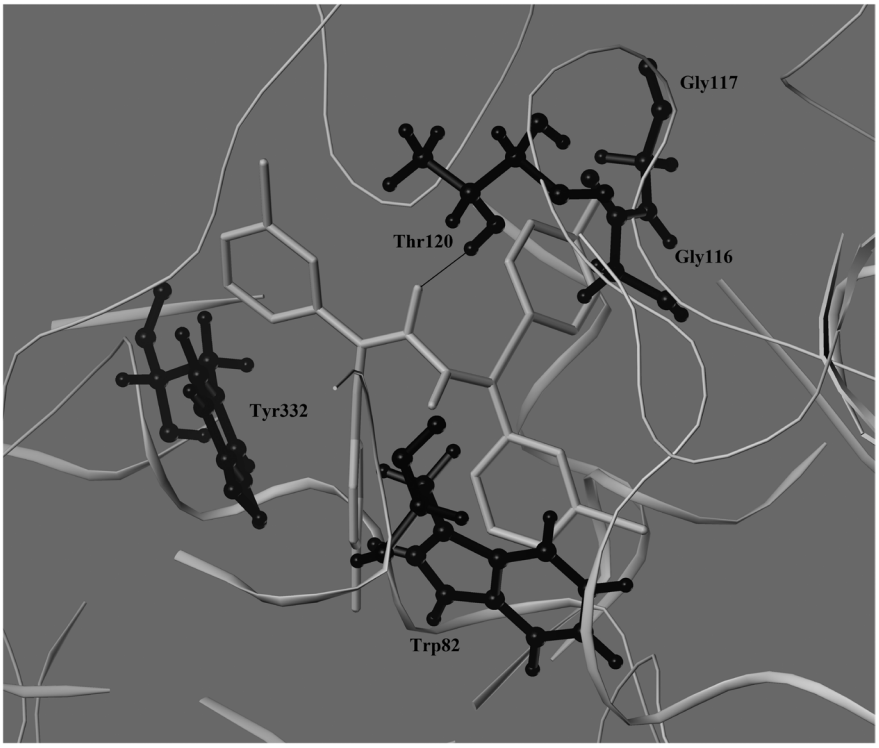

Fig. 1. Binding Interactions of Compound **1f** and HuBuChE

inhibitory activity on BuChE and among these, compound **1f**, which have a bromo substituent group on *meta* position among the ethanediamide derivatives, exhibited the strongest inhibition to BuChE with an IC_{50} value of 1.47 μM, which was 9.82- and 4.09-fold more potent than those of neostigmine (IC_{50}=14.45 μM) and ambenonium (IC_{50}=6.02 μM). In addition, the compound **1f** exhibited high BuChE inhibitor selectivity with the selectivity value of 68.02. The compound **1a**, a non-substituted derivative, showed the similar potent inhibitory activity on BuChE, with an IC_{50} of 53.76 μM. Also the other *meta*-halogenated ethanediamide derivatives, **1d** and **e**, exhibited high inhibitory activity (IC_{50}=4.78 μM and IC_{50}=3.16 μM, respectively) against BuChE (Table 1). Conversely, ethanediamide compounds were found inactive against AChE with IC_{50} values of 100 μM.

According to the activity results, the butenediamide derivatives (**2a**–**f**) were found more effective than the ethanediamide derivatives on AChE inhibition due to the ethylene bridge. This finding suggests us that the AChE inhibitory activity is strongly dependent on the presence of ethylene moiety of the chemical structure. In contrast, the ethanediamide derivatives (**1a**–**f**) were seemed as very effective inhibitors against BuChE. This finding clearly indicates that ethylene moiety especially plays an important role as AChE inhibition.

Also, the compounds were designed with different substituent groups (–H, $-CH_3$, $-C_2H_5$, –F, –Cl, –Br) on *meta* position of phenyl ring with varying electronic properties. The target compounds **1d**–**f** were found as effective inhibitors against BuChE, which have electron-withdrawing halogen atoms (–F, –Cl, –Br). This approach, as shown in Table 1, **1b**–**c** possessing an electron-donating group ($-CH_3$, $-C_2H_5$) showed a decreased BuChE inhibitory activity. It can be seen as a very similar structure activity relationship on AChE inhibition among the most potent 2-butenediamide compounds (**2d**–**f**).

Molecular Modeling Studies The binding of the most potent compounds to AChE and BuChE was performed between the most active compounds **1f** with BuChE and **2f** with AChE, using the SYBYL X 2.0. The docking results revealed that the BuChE inhibitor (**1f**) occurred a hydrogen bond interaction between the carbonyl group of the compound and OH group of Thr120 (2.04 Å) in oxyanion hole of the catalytic active site (CAS) of HuBuChE (1P0I). π–π Stacking interactions were occurred between the 3-bromo substituted phenyl ring of the compound **1f** and indole moiety of Trp82 (3.02–3.65 Å) of the peripheral anionic site (PAS) of BuChE (Fig. 1).

The most potent AChE inhibitor, compound **2f**, displayed multiple binding patterns with Torpedo californica (TcAChE-1ACJ), as shown in Fig. 2. In the 1ACJ–**2f** complex, the oxygen atom from the carbonyl group created a hydrogen bond with OH group of Ser200 (1.93 Å) into the CAS and OH group of Ser122 (1.38 Å) into the PAS. The chloro group in the *para*-positions on benzyl ring created H-bond such as the NH group of Trp84 (2.70 Å) into the CAS. The *p*-chlorobenzyl moiety of the **2f** showed a π–π stacking interaction with Phe330 (3.12–3.61 Å) into the CAS.

In order to evaluate the binding affinity and experimental IC_{50} values with some scoring functions, the most potent six molecules in series and two reference compounds were constructed and docked into the active sites of the related cholinesterase enzymes using the Surflex-dock software. Surflex-Dock score (Tscore) and consensus score (CScore) modules, which provide multiple approaches to better evaluate ligand–receptor interactions, were also used. It is hoped that by using different scoring functions, the limitations of one function may be overcome. Hence, Tscores and CScores were used as a basis to verify compounds that were expected to bind with a higher affinity. The docking scores revealed that the most potent ChE inhibitors, the compounds **1f** (Tscores [5.13] and

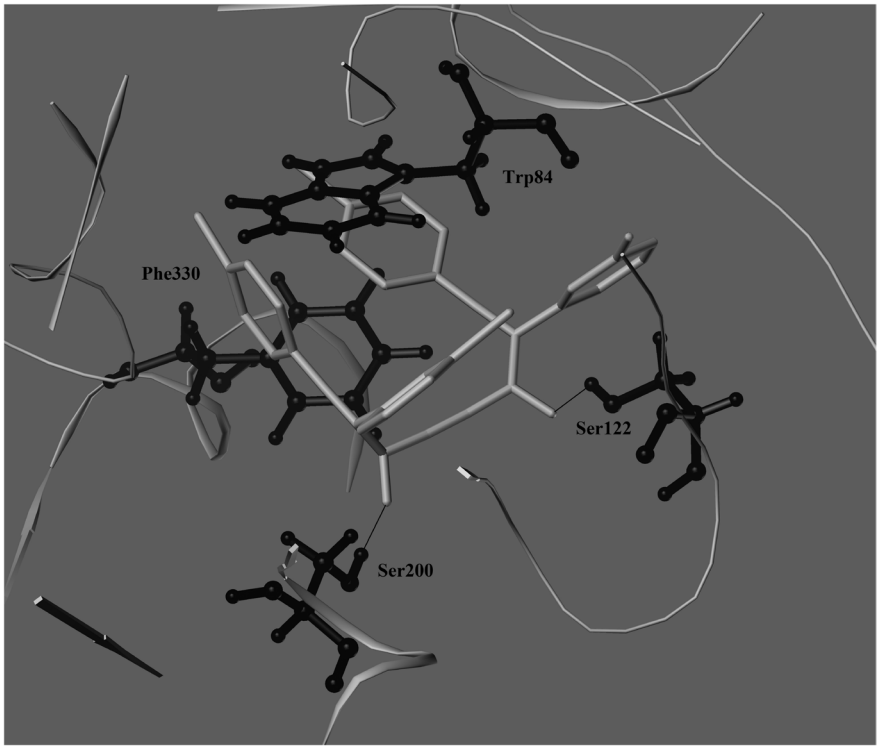

Fig. 2. Binding Interactions of Compound **2f** and TcAChE

Table 2. IC_{50} and Docking Scores of the Compounds

Compound	Docking scores of AChE						
	IC_{50} (μM)	TScore	D_Score	PMF_Score	G_Score	ChemScore	Cscore
2a	3.51	4.90	194.54	−84.07	−334.19	−58.65	3
2e	7.94	5.36	297.00	−49.12	−129.18	−41.43	3
2f	2.09	5.38	151.86	−84.26	−331.41	−59.57	4
Neostigmin	6.76	2.95	−245.25	−57.82	−140.16	−43.85	3
Ambenonium	4.07	3.51	−2001	−45.16	−361.35	−49.36	3
				Docking scores of BuChE			
1a	1.74	4.98	24.69	−39.08	−179.55	−45.41	3
1e	3.16	4.48	21.05	−44.51	−250.21	−41.45	3
1f	1.47	5.13	51.39	−65.00	−220.34	−48.26	4
Neostigmin	14.45	1.81	−383.72	−11.12	−103.53	−13.27	2
Ambenonium	6.02	1.41	−1325.36	−15.55	−152.10	−28.88	3

CScore [4]) and **2f** (Tscores [5.38] and CScore [4]) have better scores than the reference molecules. As can be seen, high Total scores and CScores parallels experimental IC_{50} quite accurately. The Tscores and CScores of all molecules are shown in Table 2.

Other scoring functions (potential of mean force (PMF), Chem, G_, and D_scores) were also used during the structure verification. These scores estimate the binding of free energy: the lower the value, the better the binding. A positive value means an unfavourable binding. Similar results were obtained when comparing these scoring functions. Briefly, all the compounds' PMF, Chem, and G_scores (except compound **2e**) report lower binding energies than those found in the reference compounds. However, examination of the other scoring functions revealed that all tested compounds, except the reference compounds, possessed positive D_scores.

Metal Chelating Effect The complexation abilities of the most potent compounds, **1f** and **2f**, for the metals such as Cu^{2+}, Fe^{2+} and Zn^{2+} in dimethylsulphoxide were studied by using UV-VIS spectrophotometer. The UV absorption of the compounds in dimethyl sulfoxide (DMSO) changed with the titration of Cu^{2+}, Fe^{2+} and Zn^{2+}. The absorption peaks of the compounds **1f** (absorbance: 0.50 at 261 nm) in DMSO increased after the addition of Cu^{2+} (absorbance: 0.78 at 262 nm) and Fe^{2+} (absorbance: 0.92 at 261 nm) (Fig. 3). The change in the absorption intensity, indicates the formation of metal chelations with Cu^{2+} and Fe^{2+} for the compound **1f.** The electronic spectra of the compound **2f** exhibited a red shift after adding Cu^{2+} (the peak at 264 nm shifted to 285 nm) and Zn^{2+} (the peak shifted to 268 nm). The other biometal, Fe^{2+}, also expressed similar result as compound **1f**–Fe^{2+} complex. The absorbance intensity of the compound **2f** (absorbance: 1.19 at 264 nm) increased when Fe^{2+} was added (absorbance: 1.32 at 263 nm) (Fig. 4).

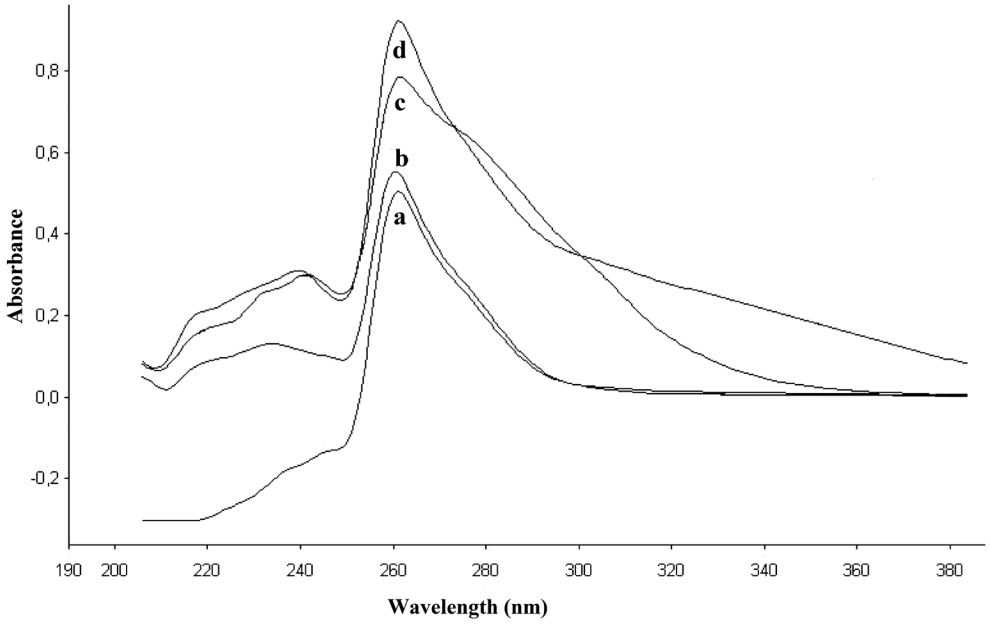

Fig. 3. (a) UV Spectrum of Compound **1f** (100 μM); (b) Spectrum of a Mixture of **1f** (100 μM) and $ZnSO_4$ (100 μM); (c) Spectrum of a Mixture of **1f** (100 μM) and $CuSO_4$; (d) Spectrum of a Mixture of **1f** (100 μM) and $FeSO_4$ (100 μM)

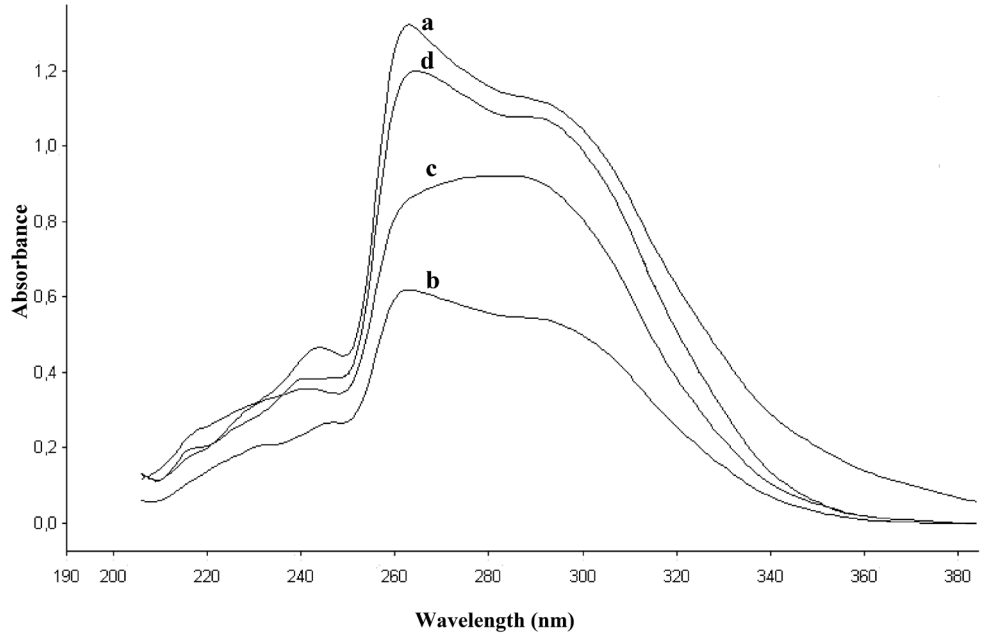

Fig. 4. (a) UV Spectrum of Compound **2f** (100 μM); (b) Spectrum of a Mixture of **2f** (100 μM) and $ZnSO_4$ (100 μM); (c) Spectrum of a Mixture of **2f** (100 μM) and $CuSO_4$; (d) Spectrum of a Mixture of **2f** (100 μM) and $FeSO_4$ (100 μM)

Conclusion

In our work, we investigated the influence of amide derivatives on AChE and BuChE inhibition activity. We explored the positive influence of the ethylene part of the 2-butenediamide derivatives (**2a**–**f**) on the AChE inhibition activity. Compound **2f**, exhibited the most potent inhibition against AChE (IC_{50} value: 2.09 μM) and good Cu^{2+}, Fe^{2+} and Zn^{2+} chelating ability. Among the synthesized ethanediamide derivatives, **1a** and **1d**–**f**, non-substituted and *meta*-halogenated derivatives, inhibited BuChE in low micromolar range, were inactive against AChE. Also the most potent ethanediamide derivative, compound **1f**, was found as the most effective inhibitor against BuChE (IC_{50} value: 1.86 μM) and good biometal (Cu^{2+}, Fe^{2+}) chelator. The docking analysis of the newly synthesized compounds, **1f** and **2f**, showed hydrogen bonding interactions with the CAS and π–π stacking interactions with the PAS of both ChEs.

Experimental

Chemistry Melting points of the compounds were obtained on Electrothermal 9100 melting-point apparatus. The ^{1}H- and ^{13}C-NMR spectra were recorded with tetra-

methylsilane (TMS) as the internal standard on a Bruker FT-400(100) MHz spectrometer using deuterated chloroform ($CDCl_3$) as the solvent. Mass spectra were recorded on Agilent 1200 mass spectrometer at 10 eV. Silica gel-G plates (Merck) were used for TLC analysis with a mixture of *n*-hexane–ethyl acetate (9 : 1). The chemical reagents and solvents used in this study were purchased from Merck or Sigma-Aldrich.

General Procedure for Synthesis of the Compounds **1(a–f)** To synthesis of the *N*,*N*′-bis-(4-chlorobenzyl)-*N*,*N*′-diaryl-oxalamide derivatives, a mixture of (4-chlorobenzyl)-(3-substituted-phenyl)-amine (1.4 mmol), triethylamine (TEA) (1.4 mmol) and oxalyl chloride (0.7 mmol) in tetrahydrofuran (10 mL) was stirred at room temperature for 12 h. The reaction mixture was quenched with 15 mL of distilled water and the aqueous phase was extracted with two portions of CH_2Cl_2. The combined organic layers were dried over Na_2SO_4, filtered and concentrated. The obtained solid was recrystallized from ethanol. Synthesis pathway is shown on Chart 1.

N,*N*′-Bis-(4-chlorobenzyl)-*N*,*N*′-diphenyl-oxalamide (**1a**) was obtained from (4-chlorobenzyl)-phenyl-amine according to general procedure as white solid. Yield 70%; mp 189–191°C. The crude compound was recrystallized from ethanol. ^{1}H-NMR (400 MHz, $CDCl_3$) δ: 4.62 (s, 4H, 2×CH_2-N), 6.66 (d, 4H, J=8.40 Hz, Ar-H), 6.87 (d, 4H, J=8.56 Hz, Ar-H), 7.06 (d, 4H, J=8.40 Hz, Ar-H), 7.31–7.27 (m, 4H, Ar-H), 7.37–7.35 (m, 2H, Ar-H). ^{13}C-NMR (100 MHz, $CDCl_3$) δ: 51.37 (CH_2-N), 128.50, 128.54, 128.60, 129.14, 129.54, 133.23, 134.81, 139.23, 164.34 (C=O). Liquid chromatography/mass spectrometry/electrospray (LC-MS-ES) (+) *m*/*z* [M+H] 489.4.

N,*N*′-Bis-(4-chlorobenzyl)-*N*,*N*′-di-*m*-tolyl-oxalamide (**1b**) was obtained from (4-chlorobenzyl)-*m*-tolyl-amine according to general procedure as white solid. Yield 24%; mp 113–115°C. The crude compound was recrystallized from ethanol. ^{1}H-NMR (400 MHz, $CDCl_3$) δ: 2.28 (s, 6H, 2×Ar-CH_3), 4.62 (s, 4H, 2×CH_2-N), 6.67 (d, 4H, J=8.28 Hz, Ar-H), 6.68 (d, 2H, J=8.76 Hz, Ar-H), 6.69 (s, 2H, Ar-H), 7.07 (d, 4H, J=8.40 Hz, Ar-H), 7.18 (m, 4H, Ar-H). ^{13}C-NMR (100 MHz, $CDCl_3$) δ: 21.25 (Ar-CH_3), 51.39 (CH_2-N), 125.44, 128.43, 128.47, 128.83, 128.90, 129.25, 129.42, 133.13, 134.99, 139.06, 164.44 (C=O). LC-MS-ES (+) *m*/*z* [M+H] 517.4.

N,*N*′-Bis-(4-chlorobenzyl)-*N*,*N*′-bis-(3-ethyl-phenyl)-oxalamide (**1c**) was obtained from (4-chlorobenzyl)-(3-ethyl-phenyl)-amine according to general procedure as white solid. Yield 14%; mp 120–123°C. The crude compound was recrystallized from ethanol. ^{1}H-NMR (400 MHz, $CDCl_3$) δ: 1.17–1.13 (t, 6H, 2×CH_2-CH_3), 2.59–2.53 (q, 4H, 2×CH_2-CH_3), 4.61 (s, 4H 2×CH_2-N), 6.62 (d, 4H, J=8.40 Hz, Ar-H), 6.70–6.68 (m, 4H, Ar-H), 7.05–7.03 (m, 6H, Ar-H), 7.21–7.19 (m, 2H, Ar-H). ^{13}C-NMR (100 MHz, $CDCl_3$) δ: 15.26 (CH_2–CH_3), 28.53 (CH_2–CH_3), 51.32 (CH_2-N), 125.72, 127.95, 128.07, 128.47, 128.89, 129.47, 133.10, 135.08, 139.28, 145.39, 164.44 (C=O). LC-MS-ES (+) *m*/*z* [M+H] 545.5.

N,*N*′-Bis-(4-chlorobenzyl)-*N*,*N*′-bis-(3-fluoro-phenyl)-oxalamide (**1d**) was obtained from (4-chlorobenzyl)-(3-fluoro-phenyl)-amine according to general procedure as white solid. Yield 34%; mp 134–137°C. The crude compound was recrystallized from ethanol. ^{1}H-NMR (400 MHz, $CDCl_3$) δ: 4.64 (s, 4H, 2×CH_2-N), 6.68–6.66 (m, 4H, Ar-H), 6.79 (d, 4H, J=8.36 Hz, Ar-H), 7.11–7.07 (m, 2H, Ar-H), 7.13 (d, 4H, J=8.36 Hz, Ar-H), 7.29–7.26 (m, 2H, Ar-H). ^{13}C-NMR (100 MHz, $CDCl_3$) δ: 51.34 (CH_2-N), 115.82 (d, $J_{C\text{-}F}$=20.7 Hz), 123.97, 124.00, 128.74, 129.63, 130.41 (d, $J_{C\text{-}F}$=9.4 Hz), 133.69, 134.33, 140.43, 140.52, 162.37 (d, $J_{C\text{-}F}$=249.7 Hz) 163.84 (C=O). LC-MS-ES (+) *m*/*z* [M+H] 525.3.

N,*N*′-Bis-(4-chlorobenzyl)-*N*,*N*′-bis-(3-chloro-phenyl)-oxalamide (**1e**) was obtained from (4-chlorobenzyl)-(3-chloro-phenyl)-amine according to general procedure as white solid. Yield 81%; mp 113–116°C. The crude compound was purified by column chromatography on SiO_2 eluting with hexane/ethyl acetate (6 : 4) and recrystallized from ethanol. ^{1}H-NMR (400 MHz, $CDCl_3$) δ: 4.62 (s, 4H, 2×CH_2-N), 6.78 (m, 6H, Ar-H), 6.83 (s, 2H, Ar-H), 7.14 (d, 4H, J=8.41 Hz, Ar-H), 7.23 (d, 2H, J=8.05 Hz, Ar-H), 7.36–7.34 (m, 2H, Ar-H). ^{13}C-NMR (100 MHz, $CDCl_3$) δ: 51.41 (CH_2-N), 126.65, 128.46, 128.77, 128.97, 129.63, 129.70, 130.20, 133.72, 134.72, 140.13, 163.79 (C=O). LC-MS-ES (+) *m*/*z* [M+H] 558.2.

N,*N*′-Bis-(3-bromo-phenyl)-*N*,*N*′-bis-(4-chlorobenzyl)-oxalamide (**1f**) was obtained from (3-bromo-phenyl)-(4-chlorobenzyl)-amine according to general procedure as white solid. Yield 69%; mp 103–106°C. The crude compound was recrystallized from ethanol. ^{1}H-NMR (400 MHz, $CDCl_3$) δ: 4.62 (s, 4H, 2×CH_2-N), 6.77 (d, 4H, J=8.40 Hz, Ar-H), 6.83 (d, 2H, J=8.00 Hz, Ar-H), 6.98 (s, 2H, Ar-H), 7.15 (d, 4H, J=8.45 Hz, Ar-H), 7.19 (d, 2H, J=8.05 Hz, Ar-H), 7.52–7.49 (m, 2H, Ar-H). ^{13}C-NMR (100 MHz, $CDCl_3$) δ: 51.34 (CH_2-N), 122.46, 127.24, 128.80, 129.62, 130.47, 131.33, 131.92, 133.73, 134.23, 140.24, 163.77 (C=O). LC-MS-ES (+) *m*/*z* [M+H] 645.8.

General Procedure for Synthesis of the Compounds **2(a–f)** A mixture of 4-(chloro-benzyl)-(3-substituted-phenyl)-amine (1.4 mmol), TEA (1.4 mmol) and dry ethylacetate (5 mL) was cooled with an ice bath to 0–5°C and fumaryl chloride (0.65 mmol) in 5 mL dry ethylacetate was added dropwise by syringe over 30 min. And the reaction mixture was stirred at room temperature for 12 h. The reaction mixture was quenched with 50 mL of water and the aqueous phase was extracted with two portions of CH_2Cl_2. The combined organic layers were dried over $MgSO_4$, filtered and concentrated by rotary evaporation. And the target compounds were recrystallized from ethanol.

But-2-enedioic Acid Bis-[(4-chlorobenzyl)-phenyl-amide] (**2a**) was obtained from (4-chlorobenzyl)-phenyl-amine according to general procedure as bright yellow. Yield 52%; mp 203–206°C. The crude compound was recrystallized from ethanol. ^{1}H-NMR (400 MHz, $CDCl_3$) δ: 4.85 (s, 4H, 2×CH_2-N), 6.86 (s, 2H, fumaryl CH=CH), 6.96 (d, 4H, J=7.88 Hz, Ar-H), 7.07 (d, 4H, J=8.32 Hz, Ar-H), 7.19 (d, 4H, J=8.32 Hz, Ar-H), 7.36–7.33 (m, 6H, Ar-H). ^{13}C-NMR (100 MHz, $CDCl_3$) δ: 52.90 (CH_2-N), 128.01, 128.43, 128.61, 129,87 130.09, 132.06 (CH=CH), 133.40, 135.41, 140.97, 164.34 (C=O). LC-MS-ES (+) *m*/*z* [M+H] 515.7.

But-2-enedioic Acid Bis-[(4-chlorobenzyl)-*m*-tolyl-amide] (**2b**) was obtained from (4-chlorobenzyl)-*m*-tolyl-amine according to general procedure as white solid. Yield 13%; mp 166–169°C. The crude compound was recrystallized from methanol. ^{1}H-NMR (400 MHz, $CDCl_3$) δ: 2.32 (s, 6H, 2×Ar-CH_3), 4.83 (s, 4H, 2×CH_2-N), 6.72 (d, 2H, J=7.72 Hz, Ar-H), 6.80 (s, 2H, Ar-H), 6.86 (s, 2H, fumaryl CH=CH), 7.08 (d, 4H, J=8.36 Hz, Ar-H), 7.13 (d, 2H, J=7.64 Hz, Ar-H), 7.21–7.19 (m, 2H, Ar-H), 7.23 (d, 4H, J=7.72 Hz, Ar-H). ^{13}C-NMR (100 MHz, $CDCl_3$) δ: 21.31 (Ar-CH_3), 52.95 (CH_2-N), 125.22, 128.37, 128.55, 129.25, 129.55, 130.07, 132.01 (CH=CH),

133.33, 135.53, 139.96, 140.96, 164.39 (*C*=*O*). LC-MS-ES (+) *m/z* [M+H] 543.5.

But-2-enedioic Acid Bis-[(4-chlorobenzyl)-(3-ethyl-phenyl)-amide] (**2c**) was obtained from (4-chlorobenzyl)-(3-ethyl-phenyl)-amine according to general procedure as white solid. Yield 32%; mp 147–150°C. The crude compound was recrystallized from ethanol. ^{1}H-NMR (400 MHz, $CDCl_3$) δ: 1.20–1.17 (t, 6H, 2×CH_2–CH_3), 2.64–2.58 (q, 4H, 2×CH_2–CH_3), 4.84 (s, 4H 2×CH_2-N), 6.75 (d, 2H, *J*=7.92 Hz, Ar-H), 6.76 (s, 2H, Ar-H), 6.87 (s, 2H, fumaryl *CH*=*CH*), 7.08 (d, 4H, *J*=8.36 Hz, Ar-H), 7.16 (d, 2H, *J*=7.70 Hz, Ar-H), 7.21–7.18 (m, 2H, Ar-H), 7.24 (d, 4H, *J*=7.64 Hz, Ar-H). ^{13}C-NMR (100 MHz, $CDCl_3$) δ: 15.26, 28.55, 52.89 (CH_2-N), 125.31, 127.26, 128.00, 128.54, 129.65, 130.12, 132.06 (*CH*=*CH*), 133.32, 135.58, 140.97, 146.21, 164.42 (*C*=*O*). LC-MS-ES (+) *m/z* [M+H] 571.6.

But-2-enedioic Acid Bis-[(4-chlorobenzyl)-(3-fluoro-phenyl)-amide] (**2d**) was obtained from (4-chlorobenzyl)-(3-fluoro-phenyl)-amine according to general procedure as white solid. Yield 34%; mp 196–199°C. The crude compound was recrystallized from ethanol. ^{1}H-NMR (400 MHz, $CDCl_3$) δ: 4.85 (s, 4H, 2×CH_2-N), 6.77–6.72 (m, 4H, Ar–H), 6.86 (s, 2H, fumaryl *CH*=*CH*), 7.08 (d, 4H, *J*=8.36 Hz, Ar-H), 7.05–7.02 (m, 2H, Ar-H), 7.22 (d, 4H, *J*=8.36 Hz, Ar-H), 7.36–7.31 (m, 2H, Ar-H). ^{13}C-NMR (100 MHz, $CDCl_3$) δ: 52.83 (CH_2-N), 115.70 (d, $J_{C\text{-}F}$=20.7 Hz), 124.05, 128.76, 130.04, 131.10 (d, $J_{C\text{-}F}$=9.3 Hz), 132.12 (*CH*=*CH*), 133.66, 134.98, 142.30, 142.39, 162.97 (d, $J_{C\text{-}F}$=249.9 Hz), 164.01 (*C*=*O*). LC-MS-ES (+) *m/z* [M+H] 551.4.

But-2-enedioic Acid Bis-[(4-chlorobenzyl)-(3-chloro-phenyl)-amide] (**2e**) was obtained from (4-chlorobenzyl)-(3-chloro-phenyl)-amine according to general procedure as white solid. Yield 55%; mp 203–205°C. The crude compound was recrystallized from ethanol. ^{1}H-NMR (400 MHz, $CDCl_3$) δ: 4.84 (s, 4H, 2×CH_2-N), 6.83–6.81 (m, 4H, Ar-H), 7.04 (s, 2H, fumaryl *CH*=*CH*), 7.08 (d, 4H, *J*=8.40 Hz, Ar-H), 7.22 (d, 4H, *J*=8.36 Hz, Ar-H), 7.28 (d, 2H, *J*=8.00 Hz, Ar-H), 7.35–7.31 (m, 2H, Ar-H). ^{13}C-NMR (100 MHz, $CDCl_3$) δ: 52.89 (CH_2-N), 126.62, 128.10, 128.76, 128.90, 130.05, 130.82, 132.14 (*CH*=*CH*), 133.68, 134.89, 135.43, 142.05, 163.98 (*C*=*O*). LC-MS-ES (+) *m/z* [M+H] 583.1.

But-2-enedioic Acid Bis-[(3-bromo-phenyl)-(4-chloro-benzyl)-amide] (**2f**) was obtained from (3-bromo-phenyl)-(4-chlorobenzyl)-amine according to general procedure as white solid. Yield 66%; mp 202–204°C. The crude compound was recrystallized from ethanol. ^{1}H-NMR (400 MHz, $CDCl_3$) δ: 4.84 (s, 4H, 2×CH_2-N), 6.83 (s, 2H, fumaryl *CH*=*CH*), 6.85 (d, 2H, *J*=8.44 Hz, Ar-H), 7.08 (d, 4H, *J*=8.36 Hz, Ar-H), 7.23–7.21 (m, 6H, Ar-H), 7.26 (s, 2H, Ar-H), 7.49 (d, 2H, *J*=8.08 Hz, Ar-H). ^{13}C-NMR (100 MHz, $CDCl_3$) δ: 52.93 (CH_2-N), 123.28, 127.13, 128.77, 130.06, 130.94, 131.06, 131.81, 132.15 (*CH*=*CH*), 133.68, 134.86, 142.17, 163.97 (*C*=*O*). LC-MS-ES (+) *m/z* [M+H] 671.3.

Pharmacology AChE, BuChE, 5,5-dithiobis-(2-nitrobenzoic acid) DTNB, acetylthiocholine iodide (ATCI) and butyrylthiocholine iodide (BTCI) were purchased from Sigma-Aldrich. Inhibitory activities of AChE and BuChE of the test compounds were evaluated by colorimetric Ellman's method[23] with some modifications using commercially available neostigmine bromide[10] and ambenonium dichloride[24] as the reference compounds. The test compounds were dissolved in dimethylsulphoxide and then diluted in 50 mM Tris buffer (pH 8.0) to provide a final concentration range. In a 96-well plate, the assay medium in each well consisted of 50 μL of a Tris buffer, 125 μL of 3 mM DTNB (Ellman's reagent), 25 μL of 0.2 U/mL enzyme (AChE or BuChE) and 15 mM substrate (ATCI or BTCI). The assay mixture containing enzyme, buffer, DTNB and 25 μL of inhibitor compound was preincubated for 15 min at 37°C, before the substrate was added to begin the reaction. Neostigmine bromide, ambenonium dichloride and all test compounds were prepared at eleven different concentrations such as 0.097, 0.195, 0.39, 0.78, 1.56, 3.13, 6.25, 12.5, 25, 50 and 100 μg/mL. The absorbance of the reaction mixture was then measured three times at 412 nm every 45 s using a microplate reader (Bio-Tek ELx800, U.S.A.). Results are presented as means±standard errors (S.E.) of the experiment. The IC_{50} values of the compounds showing percentage inhibition, the measurements and calculations were evaluated by non-linear regression analysis using GraphPad Prism software.

Chelation Capacity The metal chelation was performed in dimethylsulphoxide at room temperature using UV-Vis spectrophotometer (Thermo Electron Heλios) with wavelength ranging from 190 to 380 nm.[25,26] The UV absorption of the test compounds **1f** and **2f**, in the absence or presence of with $CuSO_4$, $FeSO_4$ and $ZnSO_4$ was recorded in a 1 cm quartz cuvette after 20 min at room temperature. The final concentrations of the test compounds and metals were 100 μM.

Molecular Docking Study In order to find out the binding mode for the synthesized compounds, docking simulation studies were carried out with Surflex-Dock. 3D structures of the compounds **1f** and **2f** were constructed using the Sybyl sketcher module. The structures were minimized using the Steepest descent conjugated gradient method until the gradient was 0.05 kcal/mol, max iterations: 1000 with the Tripos force field with the Gasteiger Huckel charge. The simulation system was built on X-ray crystallographic structures of 1ACJ and 1P0I which were obtained from the Protein Data Bank. At the commencement of docking, all the water and ligands were removed and the random hydrogen atoms were added. Docking calculations using Surflex-Dock for 1ACJ and 1P0I were performed through protomol generation by ligand. The parameters used were threshold 0.5 and bloat 0.

To evaluate the docking experiment, the Tscore,[27] D_score,[28] PMF_Score,[29] G_score,[30] and Chem-Score[31] values were estimated using the Cscore module of SYBYL X. Since Cscore is a consensus scoring function, the different scoring functions in it provide multiple approaches to better evaluate ligand–receptor interactions. The higher CScore value is associated with better promising hits.

Acknowledgment This research work was supported by Ataturk University Research Fund (Project No. 2014/167), Turkey.

Conflict of Interest The authors declare no conflict of interest.

Suppementary Materials The online version of this article contains supplementary materials.

References

1) Lambert J. C., Heath S., Even G., Campion D., Sleegers K.,

Hiltunen M., Combarros O., Zelenika D., Bullido M. J., Tavernier B., Letenneur L., Bettens K., Berr C., Pasquier F., Fiévet N., Barberger-Gateau P., Engelborghs S., De Deyn P., Mateo I., Franck A., Helisalmi S., Porcellini E., Hanon O., European Alzheimer's Disease Initiative Investigators, de Pancorbo M. M., Lendon C., Dufouil C., Jaillard C., Leveillard T., Alvarez V., Bosco P., Mancuso M., Panza F., Nacmias B., Bossù P., Piccardi P., Annoni G., Seripa D., Galimberti D., Hannequin D., Licastro F., Soininen H., Ritchie K., Blanché H., Dartigues J. F., Tzourio C., Gut I., Van Broeckhoven C., Alpérovitch A., Lathrop M., Amouyel P., *Nat. Genet.*, **41**, 1094–1099 (2009).

2) Naj A. C., Jun G., Beecham G. W., Wang L. S., Vardarajan B. N., Buros J., Gallins P. J., Buxbaum J. D., Jarvik G. P., Crane P. K., Larson E. B., Bird T. D., Boeve B. F., Graff-Radford N. R., De Jager P. L., Evans D., Schneider J. A., Carrasquillo M. M., Ertekin-Taner N., Younkin S. G., Cruchaga C., Kauwe J. S., Nowotny P., Kramer P., Hardy J., Huentelman M. J., Myers A. J., Barmada M. M., Demirci F. Y., Baldwin C. T., Green R. C., Rogaeva E., St George-Hyslop P., Arnold S. E., Barber R., Beach T., Bigio E. H., Bowen J. D., Boxer A., Burke J. R., Cairns N. J., Carlson C. S., Carney R. M., Carroll S. L., Chui H. C., Clark D. G., Corneveaux J., Cotman C. W., Cummings J. L., DeCarli C., DeKosky S. T., Diaz-Arrastia R., Dick M., Dickson D. W., Ellis W. G., Faber K. M., Fallon K. B., Farlow M. R., Ferris S., Frosch M. P., Galasko D. R., Ganguli M., Gearing M., Geschwind D. H., Ghetti B., Gilbert J. R., Gilman S., Giordani B., Glass J. D., Growdon J. H., Hamilton R. L., Harrell L. E., Head E., Honig L. S., Hulette C. M., Hyman B. T., Jicha G. A., Jin L. W., Johnson N., Karlawish J., Karydas A., Kaye J. A., Kim R., Koo E. H., Kowall N. W., Lah J. J., Levey A. I., Lieberman A. P., Lopez O. L., Mack W. J., Marson D. C., Martiniuk F., Mash D. C., Masliah E., McCormick W. C., McCurry S. M., McDavid A. N., McKee A. C., Mesulam M., Miller B. L., Miller C. A., Miller J. W., Parisi J. E., Perl D. P., Peskind E., Petersen R. C., Poon W. W., Quinn J. F., Rajbhandary R. A., Raskind M., Reisberg B., Ringman J. M., Roberson E. D., Rosenberg R. N., Sano M., Schneider L. S., Seeley W., Shelanski M. L., Slifer M. A., Smith C. D., Sonnen J. A., Spina S., Stern R. A., Tanzi R. E., Trojanowski J. Q., Troncoso J. C., Van Deerlin V. M., Vinters H. V., Vonsattel J. P., Weintraub S., Welsh-Bohmer K. A., Williamson J., Woltjer R. L., Cantwell L. B., Dombroski B. A., Beekly D., Lunetta K. L., Martin E. R., Kamboh M. I., Saykin A. J., Reiman E. M., Bennett D. A., Morris J. C., Montine T. J., Goate A. M., Blacker D., Tsuang D. W., Hakonarson H., Kukull W. A., Foroud T. M., Haines J. L., Mayeux R., Pericak-Vance M. A., Farrer L. A., Schellenberg G. D., *Nat. Genet.*, **43**, 436–441 (2011).

3) Piazzi L., Rampa A., Bisi A., Gobbi S., Belluti F., Cavalli A., Bartolini M., Andrisano V., Valenti P., Recanatini M., *J. Med. Chem.*, **46**, 2279–2282 (2003).

4) Seshadri S., Fitzpatrick A. L., Ikram M. A., DeStefano A. L., Gudnason V., Boada M., Bis J. C., Smith A. V., Carassquillo M. M., Lambert J. C., Harold D., Schrijvers E. M., Ramirez-Lorca R., Debette S., Longstreth W. T. Jr., Janssens A. C., Pankratz V. S., Dartigues J. F., Hollingworth P., Aspelund T., Hernandez I., Beiser A., Kuller L. H., Koudstaal P. J., Dickson D. W., Tzourio C., Abraham R., Antunez C., Du Y., Rotter J. I., Aulchenko Y. S., Harris T. B., Petersen R. C., Berr C., Owen M. J., Lopez-Arrieta J., Varadarajan B. N., Becker J. T., Rivadeneira F., Nalls M. A., Graff-Radford N. R., Campion D., Auerbach S., Rice K., Hofman A., Jonsson P. V., Schmidt H., Lathrop M., Mosley T. H., Au R., Psaty B. M., Uitterlinden A. G., Farrer L. A., Lumley T., Ruiz A., Williams J., Amouyel P., Younkin S. G., Wolf P. A., Launer L. J., Lopez O. L., van Duijn C. M., Breteler M. M., CHARGE Consortium, GERAD1 Consortium, EADI1 Consortium, *JAMA*, **303**, 1832–1840 (2010).

5) Singh M., Kaur M., Kukreja H., Chugh R., Silakari O., Singh D., *Eur. J. Med. Chem.*, **70**, 165–188 (2013).

6) Massoud F., Léger G., *Can. J. Psychiatry*, **56**, 579–588 (2011).

7) Winslow B. T., Onysko M., Stob C., Hazlewood K., *Am. Fam. Physician*, **83**, 1403–1412 (2011).

8) Akasofu S., Kimura M., Kosasa I., Sawada K., Ogura H., *Chem. Biol. Interact.*, **175**, 222–226 (2008).

9) Dumas J. A., Newhouse P. A., *Pharmacol. Biochem. Behav.*, **99**, 254–261 (2011).

10) Skrzypek A., Matysiak J., Niewiadomy A., Bajda M., Szymanski P., *Eur. J. Med. Chem.*, **62**, 311–319 (2013).

11) Mohamed T., Rao P., *Bioorg. Med. Chem. Lett.*, **20**, 3606–3609 (2010).

12) Bullock R., Lane R., *Curr. Alzheimer Res.*, **4**, 277–293 (2007).

13) Jhee S. S., Shiovitz T., Hartman R. D., Messina J., Anand R., Sramek J., Cutler N. R., *Clin. Neuropharmacol.*, **25**, 122–123 (2002).

14) Kamal M. A., Klein P., Luo W., Li Y., Holloway H. W., Tweedie D., Greig N. H., *Neurochem. Res.*, **33**, 745–753 (2008).

15) Mesulam M. M., Guillozet A., Shaw P., Levey A., Duysen E. G., Lockridge O., *Neuroscience*, **110**, 627–639 (2002).

16) Basiri A., Murugaiyah V., Osman H., Kumar R. S., Kia Y., Awang K. B., Ali M. A., *Eur. J. Med. Chem.*, **67**, 221–229 (2013).

17) Khoobi M., Alipour M., Moradi A., Sakhteman A., Nadri H., Razavi S. F., Ghandi M., Foroumadi A., Shafiee A., *Eur. J. Med. Chem.*, **68**, 291–300 (2013).

18) Budimir A., *Acta Pharm.*, **61**, 1–14 (2011).

19) Liu G., Huang W., Moir R. D., Vanderburg C. R., Lai B., Peng Z., Tanzi R. E., Rogers J. T., Huang X., *J. Struct. Biol.*, **155**, 45–51 (2006).

20) Zatta P., Drago D., Bolognin S., Sensi S. L., *Trends Pharmacol. Sci.*, **30**, 346–355 (2009).

21) Yerdelen K. O., Tosun E., *Med. Chem. Res.*, **24**, 588–602 (2015).

22) Yerdelen K. O., Gul H. I., *Med. Chem. Res.*, **22**, 4920–4929 (2013).

23) Ellman G. L., Courtney K. D., Andies V. Jr., Feather-stone R. M., *Biochem. Pharmacol.*, **7**, 88–95 (1961).

24) Musilek K., Komloova M., Holas O., Hrabinova M., Pohanka M., Dohnal V., Nachone F., Dolezal M., Kuca K., *Eur. J. Med. Chem.*, **46**, 811–818 (2011).

25) Huang X., Moir R. D., Tanzi R. E., Bush A. I., Rogers J. T., *Ann. N. Y. Acad. Sci.*, **1012**, 153–163 (2004).

26) Joseph R., Ramanujam B., Acharya A., Khutia A., Rao C. P., *J. Org. Chem.*, **73**, 5745–5758 (2008).

27) SYBYLX 2.0 T. I. 1699 South Hanley Rd St. Louis MO 63144 USA.

28) Kuntz I. D., Blaney J. M., Oatley S. J., Langridge R., Ferrin T. E., *J. Mol. Biol.*, **161**, 269–288 (1982).

29) Muegge I., Martin Y. C., *J. Med. Chem.*, **42**, 791–804 (1999).

30) Jones G., Willett P., Glen R. C., Leach A. R., Taylor R., *J. Mol. Biol.*, **267**, 727–748 (1997).

31) Eldridge M. D., Murray C. W., Auton T. R., Paolini G. V., Mee R. P., *J. Comput. Aided Mol. Des.*, **11**, 425–445 (1997).